Chemical Science

ROYAL SOCIETY OF CHEMISTRY

EDGE ARTICLE

View Article Online
View Journal | View Issue

Cite this: *Chem. Sci.*, 2025, **16**, 338

All publication charges for this article have been paid for by the Royal Society of Chemistry

Mechanism of ultrafast flavin photoreduction in the active site of flavoenzyme LSD1 histone demethylase†

Bo Zhuang, *[a] Rivo Ramodiharilafy,[b] Alexey Aleksandrov,*[b] Ursula Liebl[b] and Marten H. Vos *[b]

Received 9th October 2024
Accepted 24th November 2024

DOI: 10.1039/d4sc06857b

rsc.li/chemical-science

Photoreduction of oxidized flavins has a functional role in photocatalytic and photoreceptor flavoproteins. In flavoproteins without light-dependent physiological functions, ultrafast, reversible flavin photoreduction is supposedly photoprotective by nature, and holds potential for nonnatural photocatalytic applications. In this work, we combine protein mutagenesis, ultrafast spectroscopy, molecular dynamics simulations and quantum mechanics calculations to investigate the nonfunctional flavin photoreduction in a flavoenzyme, lysine-specific demethylase 1 (LSD1) which is pivotal in DNA transcription. LSD1 harbors an oxidized flavin adenine dinucleotide (FAD) cofactor and multiple electron-donating residues in the active site. Upon photoexcitation, the FAD cofactor is photoreduced in <200 fs by electron transfer (ET) from nearby residue(s), and the charge pairs recombine in *ca.* 2 ps. Site-directed mutagenesis pinpoints a specific tryptophan residue, W751, as the primary electron donor, whereas a tyrosine residue, Y761, despite being located closer to the flavin ring, does not effectively contribute to the process. Based on a hybrid quantum-classical computational approach, we characterize the W751–FAD and Y761–FAD charge-transfer states (CT_{W751} and CT_{Y761}, respectively), as well as the FAD locally excited state (LE_{FAD}), and demonstrate that the coupling between LE_{FAD} and CT_{W751} is larger than those involving CT_{Y761} by an order of magnitude, rationalizing the experimental observations. More generally, this work highlights the role of the intrinsic protein environment and details of donor–acceptor molecular configurations on the dynamics of short-range ET involving a flavin cofactor and amino acid residue(s).

Introduction

Flavins are arguably the most versatile cofactors in nature. Proteins containing flavin cofactors, named flavoproteins, are key components in a wide range of biological processes essential to life,[1–5] They have also emerged as promising tools for biotechnological applications,[3,6–9] including as photobiocatalytic tools.[10–16] Flavins can adopt multiple redox and protonation states, with the oxidized form being the most common resting state in flavoproteins.[17] Oxidized flavins absorb near-ultraviolet and blue light, and photoexcitation of flavoproteins usually leads to photoreduction of protein-bound flavins, a process that has a physiological function in some photocatalytic and photoreceptor flavoproteins. For instance, in fatty acid photodecarboxylase,[18,19] cryptochrome[20,21] and blue light using flavin (BLUF) domain,[22,23] photoreduction of a flavin cofactor by electron transfer (ET) from substrates or protein residues constitutes the primary step in their photocycles.

Photoreduction of oxidized flavins is also ubiquitous among flavoproteins that do not perform light-dependent physiological functions. In these systems, absorption of a photon induces ultrafast ET from nearby residues, typically tryptophan and tyrosine, to flavins, on a femtosecond-picosecond timescale, followed by efficient recombination of the separated charges on a picosecond timescale.[24–40] Such an ultrafast, reversible process may serve as natural photoprotective self-quenching to dissipate the photon energy, preventing undesirable photochemical reactions that may result in harmful radical species.[30,41] At the same time, this process will also impede any potential photocatalytic applications of these enzymes, as ultrafast flavin photoreduction by protein residues may outcompete productive photoreaction with external substrates. Identifying the key factors that regulate flavin photoreduction by ET from internal protein residues, as well as finding the balance between the photostability of the enzymes and their photocatalytic ability

[a]*Beijing National Laboratory for Molecular Sciences, College of Chemistry and Molecular Engineering, Peking University, 100871 Beijing, China. E-mail: zhuangbo@pku.edu.cn*

[b]*LOB, CNRS, INSERM, École Polytechnique, Institut Polytechnique de Paris, 91120 Palaiseau, France. E-mail: alexey.aleksandrov@polytechnique.edu; marten.vos@polytechnique.edu*

† Electronic supplementary information (ESI) available: Experimental and computational methods; additional results of time-resolved spectroscopic measurements and theoretical calculations. See DOI: https://doi.org/10.1039/d4sc06857b

toward external substrates, is therefore crucial for the development of new oxidized-flavin-based photobiocatalysts.[30]

In this work, we focus on the non-functional photoinduced ET processes in a flavin-dependent amine oxidase, human lysine-specific demethylase 1 (LSD1, Fig. 1A), which has multiple essential roles in mammalian biology. It harbors an oxidized flavin adenine dinucleotide (FAD) cofactor, and specifically demethylates histone lysine, thus being pivotal in regulating DNA transcription.[43–45] LSD1 is a promising molecular target for cancer therapy,[43,45] and has been found to be relevant to neurodegenerative diseases.[46,47]

The active site of LSD1 is characterized by remarkable conformational flexibility and versatile substrate- and inhibitor-binding properties, including for large compounds encompassing multiple aromatic groups.[43,48–51] This versatility in the accommodation of peptides and other large molecules may make the enzyme a suitable template for engineering other biocatalysts, including photobiocatalysts given the presence of flavin in the active site. Yet, multiple tryptophan and tyrosine residues reside in the vicinity (<8 Å) of the FAD cofactor, among which W751 and Y761 are located within van der Waals contact of FAD (Fig. 1B). As mentioned above, photoinduced ET from these residues can potentially compete with photocatalytic reactions involving external molecules in the active site.

In this context, based on femtosecond time-resolved fluorescence and transient absorption measurements on wild-type and genetically modified proteins, the present work unravels the photoinduced ET dynamics and identifies the transiently formed radical intermediates upon photoexcitation of LSD1. This approach allows us to pinpoint W751 as the primary electron donor, despite a greater donor–acceptor separation distance compared to Y761. Employing molecular dynamics (MD) simulations and hybrid quantum mechanics/molecular mechanics (QM/MM) calculations, we explore the active-site conformational dynamics of LSD1 and characterize the flavin locally excited (LE) state and the charge-transfer (CT) states involving W751 and Y761, to obtain detailed insights into the mechanism of ultrafast photoreduction of the protein-bound flavin. The implications for possible photobiocatalytic applications will be discussed.

Results and discussion

We prepared wild-type (WT) LSD1, as well as its W751F and Y761F variants, where W751 or Y761 was genetically modified to redox-inactive phenylalanine (F). The mutations slightly perturb the absorption spectrum of FAD (Fig. 1C), reflecting the changes in the electrostatic environment around FAD.[52] To investigate the configurations of FAD and nearby electron-donating residues in detail, we performed MD simulations for the LSD1 proteins. In the simulations, although the edge-to-edge distance (the shortest distance between any non-hydrogen atoms from two aromatic rings) from residues Y571 and W695 to FAD displays broader distributions in the mutated proteins, the distances from W751

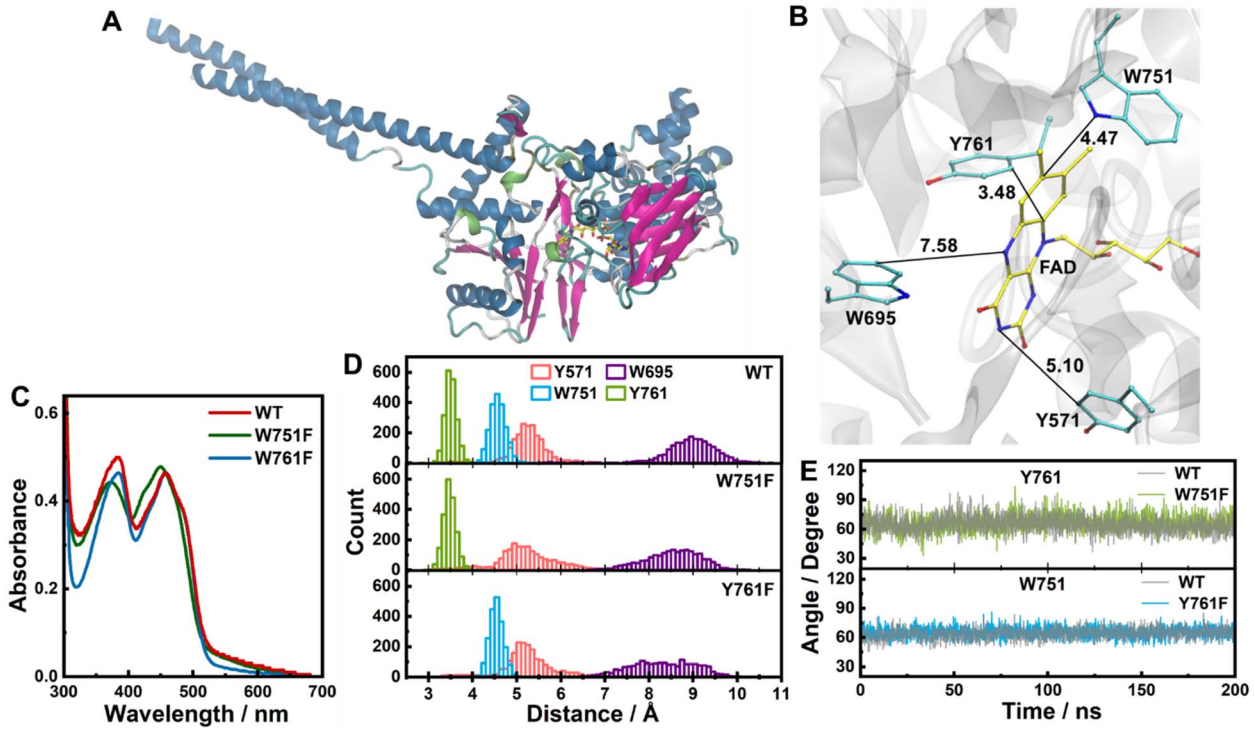

Fig. 1 (A) X-ray crystallographic structure of WT LSD1 (PDB entry: 2DW4).[42] (B) Electron-donating residues in the active site of WT LSD1 in the crystal structure (distances given in Å). (C) Steady-state absorption spectra of WT, W751F and Y761F LSD1. (D) Distributions of the edge-to-edge distances between FAD and close-by tyrosine and tryptophan residues in 200 ns MD simulations. (E) Dynamics of the angles between the ring planes of the isoalloxazine moiety of FAD and the indole or phenol moiety of Y761 or W751, during the MD simulations of WT, W751F and Y761F LSD1, as indicated.

and Y761 to FAD in W751F and Y761F LSD1 remain similar to those of WT LSD1, with average distances of 3.4 and 4.5 Å, respectively (Fig. 1D and S1†). The orientations of W751 or Y761 are largely unaffected by the mutations as well (Fig. 1E), although modest increases in the angles between the ring planes were observed (Fig. S2†). These results indicate that, although the mutations introduce changes in the protein active site, W751 and Y761 remain in close interaction with FAD in the corresponding variants. Notably, Y761 exhibits higher flexibility than W751, which can be associated with the functional role of Y761 in the accommodation of substrates.[53]

To examine the excited-state dynamics, we performed time-resolved fluorescence measurements with femtosecond time resolution on the LSD1 proteins. As shown in Fig. 2, the characteristic emission spectra of FAD centered at *ca.* 525 nm were clearly resolved. In WT and Y761F LSD1, the fluorescence decays predominantly in *ca.* 180 and 270 fs, respectively (Fig. 2A, C, and Table S1†). Such short lifetimes of the singlet excited state of FAD (FAD*, *i.e.*, the LE state of FAD) are indicative of quenching by ultrafast ET from nearby residue(s). On the other hand, an overall much slower, biexponential, fluorescence decay was detected in W751F LSD1, with time constants of 9 ps and 200 ps (Fig. 2B), an order of magnitude slower than WT and Y761F LSD1.

To characterize the formation of photoproducts and the subsequent charge recombination processes, we further performed transient absorption (TA) measurements on the LSD1 proteins. Fig. 3A shows the TA spectra of WT, W751F, and Y761F LSD1 recorded 3 ps after excitation. The evolution-associated spectra (EAS), obtained from global analysis of the TA data assuming linear reaction schemes, are given in Fig. S3.† These results can be compared with the reference TA spectra of the transient species involved in photochemical processes of FAD obtained in FNR proteins from *Bacillus subtilis* (*Bs*FNR; Fig. S4†).[27]

In all three LSD1 proteins, the negative bands at *ca.* 450 nm are dominated by the ground-state bleaching of FAD (*cf.* Fig. 1B). The TA spectra of WT LSD1 and Y761F LSD1 are further characterized by induced absorption bands peaking at *ca.* 600 nm, which correspond well to the spectrum of transient $W^{\bullet+}$ species in an unrelaxed protein environment, and the spectral features of FAD* are clearly absent (Fig. S4†).[27] Additionally, the TA spectrum of WT LSD1 does not contain apparent contributions of $Y^{\bullet+}$.[27,38] Altogether, this demonstrates the ultrafast flavin photoreduction and the formation of a $W^{\bullet+}/FAD^{\bullet-}$ radical pair as the photoproduct. The TA spectrum of W751F LSD1, by contrast, is characterized by a marked dip at *ca.* 570 nm, which resembles a stimulated emission (SE) feature, but is superimposed on a broad induced absorption band. Further spectral analysis suggests that a mixture of FAD* and a $W^{\bullet+}/FAD^{\bullet-}$ radical pair can best reproduce the observed spectral features. (Fig. S5†). The persistence of FAD* for up to hundreds of

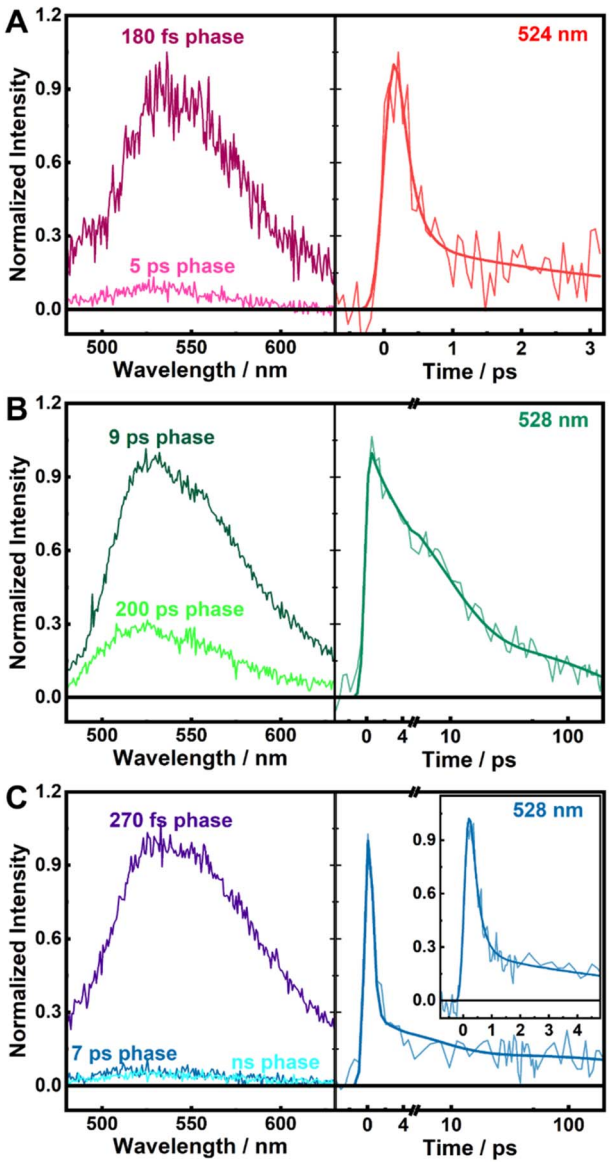

Fig. 2 Decay associated spectra (DAS) from the global analysis of fluorescence decays (left) and kinetic traces at selected wavelengths (right) of WT (A), W751F (B, linear-logarithmic time scale), and Y761F (C, linear-logarithmic time scale; inset shows a zoom of the time range of a few picoseconds) LSD1, with 390 nm excitation.

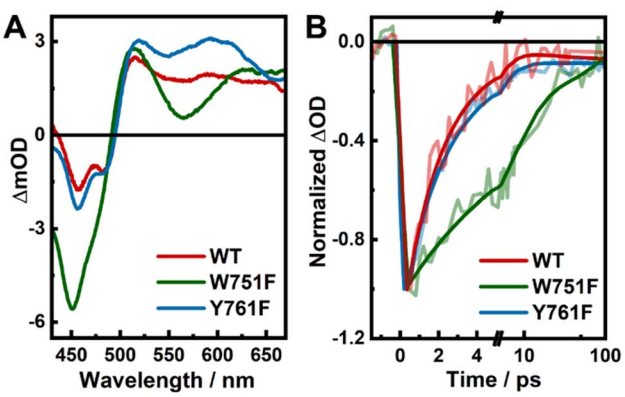

Fig. 3 Transient absorption spectra of LSD1 variants measured at 3 ps after excitation (A), and normalized kinetic traces at 460 nm (B), with 390 nm excitation.

picoseconds upon the excitation of W751F LSD1 is consistent with the time-resolved fluorescence measurement (Fig. 2B).

The TA kinetic traces probed at 460 nm (Fig. 3B) represent the recovery of ground-state FAD through charge recombination. In WT and Y761F LSD1, the separated charges mainly recombine in *ca.* 2 ps, with additional minor slower components (Fig. 3B and S3a and c†), which may be due to protein heterogeneity or the presence of a small fraction of unbound FAD, but were too small to be reliably analyzed (<1% of the initial bleaching signals). In W751F LSD1, the GSB signal displays a slow, multiphasic recovery, with fitted lifetimes of 6 and 250 ps (similar to those found in the fluorescence decay), as well as a long-lived component that was most likely due to the FAD triplet state (Fig. S3b†).

Taken together, our spectroscopic data point to W751 as a more effective electron donor than Y761, for the following reasons. First, in W751F LSD1, in the absence of W751, FAD* decays on a much longer, picosecond timescale compared to WT LSD1, and a more distant tryptophan, most likely W695 (Fig. 1B, D and S5†) is involved in the quenching process. Second, in Y761F LSD1, W751 quenches FAD* predominantly in 270 fs, close to the main fluorescence decay of WT LSD1 (Fig. 2A, C, and Table S1†), and in both systems, the $W^{\bullet+}/FAD^{\bullet-}$ radical pair accumulates as the photoproduct (Fig. 3A). Additionally, In WT and Y761F, sequential ET beyond W751 is unlikely to occur, as other tryptophan and tyrosine residues (including Y761) are all located too far away (>8 Å) from W751 to allow further ET that can outcompete the picosecond charge recombination process (Fig. 3B).

Despite being a less effective quencher, Y761 is located closer to the flavin ring of FAD than W751 in LSD1 (*ca.* 3.5 Å *versus* 4.5 Å; Fig. 1B and D). Reportedly in other flavoprotein systems, such as *Bs*FNR[27] and flavodoxin from *Helicobacter pylori* (*Hp*Fd),[37] a tyrosine residue located at a similar distance (*ca.* 3.5 Å) from the flavin cofactor quenches the flavin excited state in *ca.* 200 fs, comparable to those in WT and Y761F LSD1. It is intriguing to note that Y761 does not effectively participate in the quenching process in competition with W751. To obtain a rationale behind this observation, we adopted a QM/MM approach to investigate the photoinduced ET in LSD1, by estimating the energy levels of and the coupling between relevant electronic states, *i.e.*, the FAD LE state and CT states involving W751 and Y761.

Specifically, the QM region, which was described at a density functional theory (DFT) level, included the flavin (isoalloxazine) ring of FAD, as well as the side chains of W751 and Y761, while the remaining part of the protein and water molecules were described by classical force fields. As the dynamics of photoinduced short-range ET in proteins are assumed to be faster than the local relaxation, the protein environment can be considered 'frozen' during the ET process, with a heterogeneous distribution of electrostatics that can reasonably be sampled from ground-state MD simulations.[27,35,54] Therefore, we carried out time-dependent DFT (TDDFT) calculations along the ground-state MD trajectories after DFT geometry optimizations of the QM regions. Hole–electron analysis was further performed to reveal the underlying characteristics of the excited state, which described the changes in electron density upon the corresponding electronic excitation;[55] in a typical LE state, the hole and electron are both localized on the flavin ring of FAD, and in a well-defined CT state the transferred electron is localized on the flavin ring, and the hole is localized on the donor (*i.e.*, W751 or Y761 in LSD1).

As shown in Fig. 4A–C, two excited states with distinct CT characters and energy levels lower than that of the FAD LE state (corresponding to the $S_0 \rightarrow S_1$ transition of FAD; hereafter referred to as LE_{FAD}) were identified. CT_{Y761} involves ET from Y761 to FAD and CT_{W751} involves ET from W751 to FAD, as evident from the corresponding hole–electron distributions. The oscillator strengths of LE_{FAD} have values of *ca.* 0.19 (Table S2†), indicating that they can be populated directly by photoexcitation. By contrast, the CT states cannot be accessed directly, as the oscillator strengths of these transitions are virtually zero. These findings are consistent with the ultrafast experiments in which photoinduced charge separation in LSD1 is achieved following the decay of FAD* (Fig. 2 and 3). Notably, the energy levels of the CT_{Y761} are slightly lower than CT_{W751} (Fig. 4D; with averaged values of 2.02 and 2.25 eV respectively), contradicting the general assumption that ET from tryptophan is energetically favorable compared to tyrosine in flavoproteins.[56] As the CT states are close in energy, the ET dynamics should be predominantly determined by the electronic coupling matrix (H_{ab}) between the LE and CT states, which depends on the overlap of the wave functions of relevant electronic states, and is sensitive to the relative molecular configuration and distance of the donor and acceptor molecules. Specifically, we estimated H_{ab} with the two-state generalized Mulliken–Hush (GMH) approximation (eqn (S1†)).[54,57–59] As shown in Fig. 4E and Table S2,† the H_{ab} between LE_{FAD} and CT_{W751} are an order of magnitude larger than those between LE_{FAD} and CT_{Y761}. As larger coupling leads to a higher ET rate (which approximately scales with $|H_{ab}|^2$), this rationalizes our experimental finding that W751 is a more effective electron donor in ultrafast flavin photoreduction in WT LSD1 than Y761. Additionally, in the simulations of W751F and Y761F LSD1, LE_{FAD}, CT_{W751} and CT_{Y761} states with hole–electron distributions similar to those in WT LSD1 were identified (Fig. S6†). It is worth noting that in Y761F, on average a slightly smaller H_{ab} between LE_{FAD} and CT_{W751} was observed compared to that in WT LSD (5.92 and 6.42 meV, respectively). This finding is fully in line with the slightly faster quenching of FAD* observed in WT LSD1 compared to Y761F LSD1 (Fig. 2A, C, and Table S1†).

We also found that subtle changes in the donor–acceptor configurations (Fig. 1D and E) can lead to considerable differences in H_{ab} (Fig. 4E, and S8†). Specifically, we found that for Y761 in WT LSD1, shorter distances and smaller angles correlate well with larger H_{ab} values (Fig. S9a and S10†). For W751, however, while there appears to be a similar trend, the correlation is less evident (Fig. S9b and S10†). This may be due to the fact that W751 is located farther away from the flavin ring (Fig. 1B), and considerably less flexible than Y761 (Fig. 1D, E, S1 and S2†), with the distances and angles fluctuating in relatively small ranges (Fig. S10†), possibly in a regime where the effects of distances and angles, as well as the contributions from surrounding protein environment, are coupled in a complex

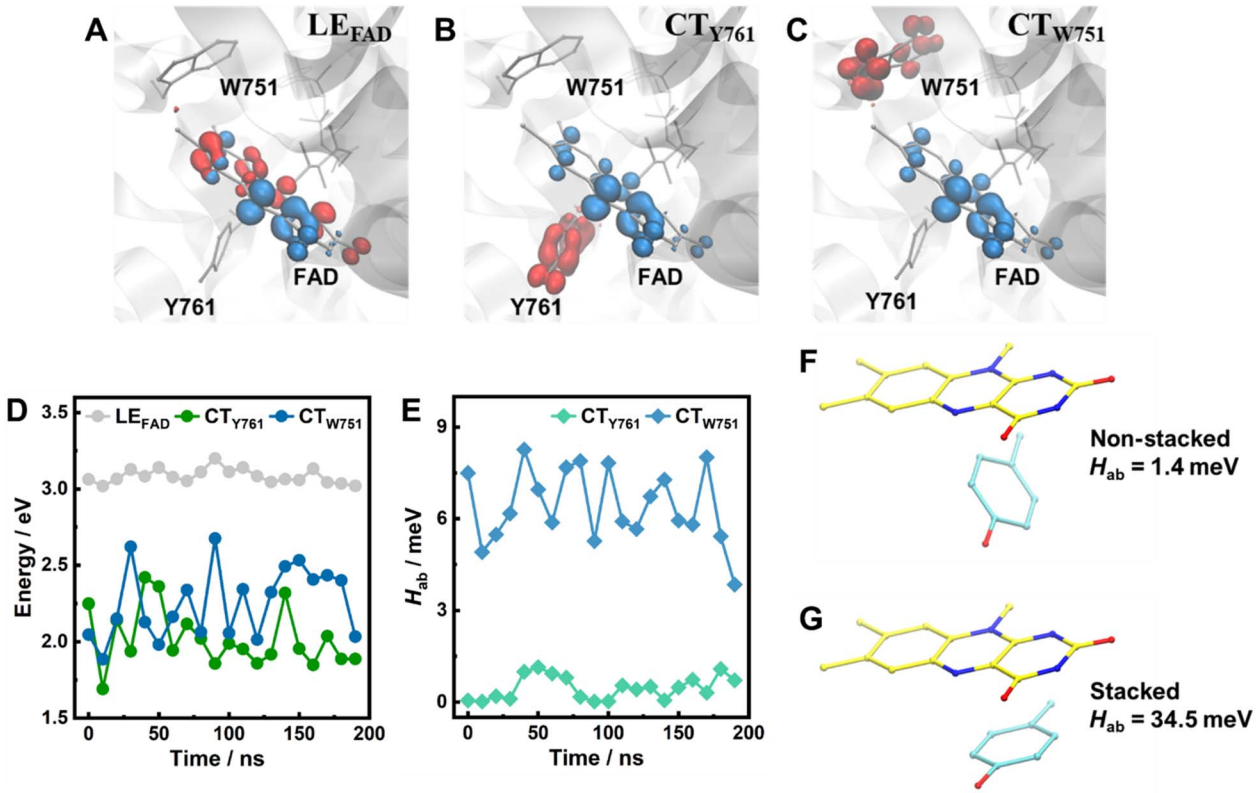

Fig. 4 (A–C) Hole–electron distributions of the FAD LE state (A), the lowest-lying CT states involving Y761 (B) and W751 (C). Red and blue regions denote the hole and electron distributions, respectively (isovalue = 0.004). Hydrogen atoms are not shown for clarity. (D and E) The energy levels of these states (D), with respect to the electronic ground state, as well as the electronic couplings between the LE and CT states in WT LSD1 (E), along the MD trajectories. (F and G) Calculated electronic coupling between flavin LE state and tyrosine–flavin CT state in non-stacked (F) and stacked (G) donor–acceptor configurations but with similar separation distance (*ca.* 4 Å). Hydrogen atoms are not shown for clarity.

manner. The fluctuations in H_{ab} explain the multiphasic fluorescence decay kinetics (Fig. 2). Moreover, the results for Tyr761 (Fig. S9a and S10†) suggest that a smaller angle between the ring planes corresponds to a larger H_{ab} value, in line with the observation that, in *Bs*FNR and *Hp*Fd, the sub-picosecond quenching events involve tyrosine residues that are stacked with the flavin rings.[27,37] It has been demonstrated in various systems that a cofacial arrangement of an aromatic donor–acceptor pair can enhance the coupling and consequently expedite ET,[60–62] Here, we applied TDDFT calculations on a simplified tyrosine–flavin model system (Fig. 4F and G) to further examine such an assessment. The result demonstrates that when a tyrosine residue is present in a stacking configuration, H_{ab} is greater than that obtained for a non-stacking configuration by more than an order of magnitude (1.4 *versus* 34.5 meV), confirming that a stacking donor–acceptor configuration is more favorable for short-range ET between a flavin and a tyrosine residue.

Finally, our findings have implications for potential use of modified LSD1 as a photobiocatalyst. Flavoprotein-based photocatalysts often (but not always) are active in the fully reduced state of the protein. They can be brought into this quasi-stable state by flavin photoreduction in the presence of sacrificial electron donors.[63] The very efficient (*ca.* 180 fs), reversible intraprotein ET between W751 and the flavin competes with such a reaction in WT LSD1. This competing flavin photoreduction reaction is slowed down by almost two orders of magnitude upon replacement of W751 with phenylalanine. At this point, quasi-stable photoreduction by external electron donors, which has been reported to be able to occur as fast as *ca.* 1 ps when accommodated in the active site of flavoproteins,[64] is likely to become sizeable. Interestingly, and *a priori* unexpectedly, the Y761 residue, also a potential electron donor to excited flavin, does not significantly contribute to the intra-protein photoinduced ET despite its closeness. As this residue plays an important role in accommodation of the peptidic substrate,[53] its photochemical inertness may be favorable for peptide photobiocatalysis. Future work will explore these issues experimentally.

Conclusions

Combining comprehensive experimental and computational approaches, we delved into the dynamics and mechanism of the ultrafast flavin photoreduction in LSD1. Based on ultrafast spectroscopic measurements on wild-type and genetically modified proteins, we demonstrated that FAD* in WT LSD1 was quenched in <200 fs by short-range ET from nearby residues, where W751 emerged as the dominant electron donor despite a greater donor–acceptor separation distance than that of

a tyrosine residue, Y761, located closer to the flavin ring. Calculations based on a QM/MM approach allowed us to characterize the LE and CT states of the FAD/W/Y system in the protein active sites, where we found that the electronic coupling between the FAD LE state and the CT state involving W751 is greater than that involving Y761 by an order of magnitude, corroborating our experimental findings. By examining the effects of donor–acceptor configurations on the electronic coupling between the LE and CT states, we further showed that a stacking configuration of the tyrosine–flavin pair was required for short-range photoinduced ET to efficiently occur. Taken together, our results provide detailed insights into the ultrafast flavin photoreduction in an intricate protein environment, which helps understand similar features in many other flavoprotein systems and may guide potential photobiocatalytic applications.

Data availability

The data supporting this study are available within the article and ESI.† The raw data are available from the corresponding authors upon reasonable request.

Author contributions

B. Z.: methodology, investigation, data analysis, visualization, writing – original draft preparation, writing – reviewing and editing; R. R.: methodology; A. A.: methodology, investigation, writing – reviewing and editing; U. L.; conceptualization, methodology, writing – reviewing and editing; M. H. V.: conceptualization, methodology, investigation, data analysis, writing – reviewing and editing.

Conflicts of interest

There are no conflicts to declare.

Acknowledgements

This work is partly supported by Beijing Natural Science Foundation (Grant Number 2244070) and China Postdoctoral Science Foundation (Grant Number 2024M750080).

Notes and references

1 S. Ghisla and V. Massey, *Eur. J. Biochem.*, 1989, **181**, 1–17.
2 C. T. Walsh and T. A. Wencewicz, *Nat. Prod. Rep.*, 2012, **30**, 175–200.
3 W. P. Dijkman, G. De Gonzalo, A. Mattevi and M. W. Fraaije, *Appl. Microbiol. Biotechnol.*, 2013, **97**, 5177–5188.
4 W. Buckel and R. K. Thauer, *Chem. Rev.*, 2018, **118**, 3862–3886.
5 B. J. Henriques, R. Katrine Jentoft Olsen, C. M. Gomes and P. Bross, *Gene*, 2021, **776**, 145407.
6 S. Chapman, C. Faulkner, E. Kaiserli, C. Garcia-Mata, E. I. Savenkov, A. G. Roberts, K. J. Oparka and J. M. Christie, *Proc. Natl. Acad. Sci. U. S. A.*, 2008, **105**, 20038–20043.
7 J. M. Christie, J. Gawthorne, G. Young, N. J. Fraser and A. J. Roe, *Mol. Plant*, 2012, **5**, 533–544.
8 A. P. Ryumina, E. O. Serebrovskaya, M. V. Shirmanova, L. B. Snopova, M. M. Kuznetsova, I. V. Turchin, N. I. Ignatova, N. V. Klementieva, A. F. Fradkov, B. E. Shakhov, E. V. Zagaynova, K. A. Lukyanov and S. A. Lukyanov, *Biochim. Biophys. Acta, Gen. Subj.*, 2013, **1830**, 5059–5067.
9 C. E. Paul, D. Eggerichs, A. H. Westphal, D. Tischler and W. J. H. van Berkel, *Biotechnol. Adv.*, 2021, **51**, 107712.
10 K. F. Biegasiewicz, S. J. Cooper, X. Gao, D. G. Oblinsky, J. H. Kim, S. E. Garfinkle, L. A. Joyce, B. A. Sandoval, G. D. Scholes and T. K. Hyster, *Science*, 2019, **364**, 1166–1169.
11 L. Schmermund, V. Jurkaš, F. F. Özgen, G. D. Barone, H. C. Büchsenschütz, C. K. Winkler, S. Schmidt, R. Kourist and W. Kroutil, *ACS Catal.*, 2019, **9**, 4115–4144.
12 L. E. Meyer, B. E. Eser and S. Kara, *Curr. Opin. Green Sustain. Chem.*, 2021, **31**, 100496.
13 A. Taylor, D. J. Heyes and N. S. Scrutton, *Curr. Opin. Struct. Biol.*, 2022, **77**, 102491.
14 W. Harrison, X. Huang and H. Zhao, *Acc. Chem. Res.*, 2022, **55**, 1087–1096.
15 M. A. Emmanuel, S. G. Bender, C. Bilodeau, J. M. Carceller, J. S. DeHovitz, H. Fu, Y. Liu, B. T. Nicholls, Y. Ouyang, C. G. Page, T. Qiao, F. C. Raps, D. R. Sorigué, S. Z. Sun, J. Turek-Herman, Y. Ye, A. Rivas-Souchet, J. Cao and T. K. Hyster, *Chem. Rev.*, 2023, **123**, 5459–5520.
16 W. Z. Ng, E. S. Chan, W. Gourich, C. W. Ooi, B. T. Tey and C. P. Song, *Renew. Sustain. Energy Rev.*, 2023, **184**, 113548.
17 R. Miura, *Chem. Rec.*, 2001, **1**, 183–194.
18 D. Sorigué, B. Légeret, S. Cuiné, S. Blangy, S. Moulin, E. Billon, P. Richaud, S. Brugière, Y. Couté, D. Nurizzo, P. Müller, K. Brettel, D. Pignol, P. Arnoux, Y. Li-Beisson, G. Peltier and F. Beisson, *Science*, 2017, **357**, 903–907.
19 D. Sorigué, K. Hadjidemetriou, S. Blangy, G. Gotthard, A. Bonvalet, N. Coquelle, P. Samire, A. Aleksandrov, L. Antonucci, A. Benachir, S. Boutet, M. Byrdin, M. Cammarata, S. Carbajo, S. Cuiné, R. B. Doak, L. Foucar, A. Gorel, M. Grünbein, E. Hartmann, R. Hienerwadel, M. Hilpert, M. Kloos, T. J. Lane, B. Légeret, P. Legrand, Y. Li-Beisson, S. L. Y. Moulin, D. Nurizzo, G. Peltier, G. Schirò, R. L. Shoeman, M. Sliwa, X. Solinas, B. Zhuang, T. R. M. Barends, J.-P. Colletier, M. Joffre, A. Royant, C. Berthomieu, M. Weik, T. Domratcheva, K. Brettel, M. H. Vos, I. Schlichting, P. Arnoux, P. Müller and F. Beisson, *Science*, 2021, **372**, eabd5687.
20 F. Lacombat, A. Espagne, N. Dozova, P. Plaza, P. Müller, K. Brettel, S. Franz-Badur and L. O. Essen, *J. Am. Chem. Soc.*, 2019, **141**, 13394–13409.
21 Q. Wang and C. Lin, *Annu. Rev. Plant Biol.*, 2020, **71**, 103–129.
22 A. Lukacs, R. Brust, A. Haigney, S. P. Laptenok, K. Addison, A. Gil, M. Towrie, G. M. Greetham, P. J. Tonge and S. R. Meech, *J. Am. Chem. Soc.*, 2014, **136**, 4605–4615.
23 A. Lukacs, P. J. Tonge and S. R. Meech, *Acc. Chem. Res.*, 2022, **55**, 402–414.

24 N. Mataga, H. Chosrowjan, Y. Shibata, F. Tanaka, Y. Nishina and K. Shiga, *J. Phys. Chem. B*, 2000, **104**, 10667–10677.
25 D. Zhong and A. H. Zewail, *Proc. Natl. Acad. Sci. U.S.A.*, 2001, **98**, 11867–11872.
26 B. Kudisch, D. G. Oblinsky, M. J. Black, A. Zieleniewska, M. A. Emmanuel, G. Rumbles, T. K. Hyster and G. D. Scholes, *J. Phys. Chem. B*, 2020, **124**, 11236–11249.
27 B. Zhuang, D. Seo, A. Aleksandrov and M. H. Vos, *J. Am. Chem. Soc.*, 2021, **143**, 2757–2768.
28 J. Yang, Y. Zhang, T. F. He, Y. Lu, L. Wang, B. Ding and D. Zhong, *Phys. Chem. Chem. Phys.*, 2021, **24**, 382–391.
29 B. Zhuang, L. Nag, P. Sournia, A. Croitoru, R. Ramodiharilafy, J.-C. Lambry, H. Myllykallio, A. Aleksandrov, U. Liebl and M. H. Vos, *Photochem. Photobiol. Sci.*, 2021, **20**, 663–670.
30 B. Zhuang, U. Liebl and M. H. Vos, *J. Phys. Chem. B*, 2022, **126**, 3199–3207.
31 B. Zhuang, M. H. Vos and A. Aleksandrov, *ChemBioChem*, 2022, **23**, e202200227.
32 Y. Zhang, J. Yang, N. Liu, L. Wang, F. Lu, J. Chen and D. Zhong, *J. Phys. Chem. Lett.*, 2023, **14**, 10657–10663.
33 N. Mataga, H. Chosrowjan, S. Taniguchi, F. Tanaka, N. Kido and M. Kitamura, *J. Phys. Chem. B*, 2002, **106**, 8917–8920.
34 H. Chosrowjan, S. Taniguchi, N. Mataga, F. Tanaka, D. Todoroki and M. Kitamura, *Chem. Phys. Lett.*, 2008, **462**, 121–124.
35 T. F. He, L. Guo, X. Guo, C. W. Chang, L. Wang and D. Zhong, *Biochemistry*, 2013, **52**, 9120–9128.
36 S. P. Laptenok, L. Bouzhir-Sima, J. C. Lambry, H. Myllykallio, U. Liebl and M. H. Vos, *Proc. Natl. Acad. Sci. U. S. A.*, 2013, **110**, 8924–8929.
37 K. Lugsanangarm, S. Pianwanit, A. Nueangaudom, S. Kokpol, F. Tanakaa, N. Nunthaboot, K. Ogino, R. Takagi, T. Nakanishic, M. Kitamura, S. Taniguchi and H. Chosrowjan, *J. Photochem. Photobiol. A Chem.*, 2013, **268**, 58–66.
38 L. Nag, P. Sournia, H. Myllykallio, U. Liebl and M. H. Vos, *J. Am. Chem. Soc.*, 2017, **139**, 11500–11505.
39 L. Nag, A. Lukacs and M. H. Vos, *ChemPhysChem*, 2019, **20**, 1793–1798.
40 N. Dozova, F. Lacombat, C. Bou-Nader, D. Hamdane and P. Plaza, *Phys. Chem. Chem. Phys.*, 2019, **21**, 8743–8756.
41 S. Ernst, S. Rovida, A. Mattevi, S. Fetzner and S. L. Drees, *Nat. Commun.*, 2020, **11**, 1–11.
42 S. Mimasu, T. Sengoku, S. Fukuzawa, T. Umehara and S. Yokoyama, *Biochem. Biophys. Res. Commun.*, 2008, **366**, 15–22.
43 Y. C. Zheng, J. Ma, Z. Wang, J. Li, B. Jiang, W. Zhou, X. Shi, X. Wang, W. Zhao and H. M. Liu, *Med. Res. Rev.*, 2015, **35**, 1032–1071.
44 A. Maiques-Diaz and T. C. P. Somervaille, *Epigenomics*, 2016, **8**, 1103–1116.
45 X. Zhang, X. Wang, T. Wu, W. Yin, J. Yan, Y. Sun and D. Zhao, *Pharmacol. Res.*, 2022, **175**, 105958.
46 A. K. Engstrom, A. C. Walker, R. A. Moudgal, D. A. Myrick, S. M. Kyle, Y. Bai, M. Jordan Rowley and D. J. Katz, *Proc. Natl. Acad. Sci. U. S. A.*, 2020, **117**, 29133–29143.
47 Y. Li, Y. Zhao, X. Li, L. Zhai, H. Zheng, Y. Yan, Q. Fu, J. Ma, H. Fu, Z. Zhang and Z. Li, *Front. Pharmacol*, 2022, **13**, 1020556.
48 Y. Chen, Y. Yang, F. Wang, K. Wan, K. Yamane, Y. Zhang and M. Lei, *Proc. Natl. Acad. Sci. U. S. A.*, 2006, **103**, 13956–13961.
49 F. Forneris, C. Binda, M. A. Vanoni, E. Battaglioli and A. Mattevi, *J. Biol. Chem.*, 2005, **280**, 41360–41365.
50 X. J. Dai, Y. Liu, L. P. Xue, X. P. Xiong, Y. Zhou, Y. C. Zheng and H. M. Liu, *J. Med. Chem.*, 2021, **64**, 2466–2488.
51 B. Noce, E. Di Bello, R. Fioravanti and A. Mai, *Front. Pharmacol.*, 2023, **14**, 1120911.
52 M. P. Kabir, D. Ouedraogo, Y. Orozco-Gonzalez, G. Gadda and S. Gozem, *J. Phys. Chem. B*, 2023, **127**, 1301–1311.
53 M. Yang, J. C. Culhane, L. M. Szewczuk, C. B. Gocke, C. A. Brautigam, D. R. Tomchick, M. MacHius, P. A. Cole and H. Yu, *Nat. Struct. Mol. Biol.*, 2007, **14**, 535–539.
54 F. Cailliez, P. Müller, M. Gallois and A. De La Lande, *J. Am. Chem. Soc.*, 2014, **136**, 12974–12986.
55 Z. Liu, T. Lu and Q. Chen, *Carbon N. Y.*, 2020, **165**, 461–467.
56 F. Tanaka, R. Rujkorakarn, H. Chosrowjan, S. Taniguchi and N. Mataga, *Chem. Phys.*, 2008, **348**, 237–241.
57 R. J. Cave and M. D. Newton, *Chem. Phys. Lett.*, 1996, **249**, 15–19.
58 R. J. Cave and M. D. Newton, *J. Chem. Phys.*, 1997, **106**, 9213–9226.
59 T. Kastinen, D. A. Da Silva Filho, L. Paunonen, M. Linares, L. A. Ribeiro Junior, O. Cramariuc and T. I. Hukka, *Phys. Chem. Chem. Phys.*, 2019, **21**, 25606–25625.
60 D. M. Guldi, C. Luo, M. Prato, A. Troisi, F. Zerbetto, M. Scheloske, E. Dietel, W. Bauer and A. Hirsh, *J. Am. Chem. Soc.*, 2001, **123**, 9166–9167.
61 A. Gouloumis, D. González-Rodríguez, P. Vázquez, T. Torres, S. Liu, L. Echegoyen, J. Ramey, G. L. Hug and D. M. Guldi, *J. Am. Chem. Soc.*, 2006, **128**, 12674–12684.
62 C. Jiang, J. Miao, D. Zhang, Z. Wen, C. Yang and K. Li, *Research*, 2022, **2022**, 9892802.
63 F. C. Raps, A. Rivas-Souchet, C. M. Jones and T. K. Hyster, *Nature*, 2024, DOI: **10.1038/s41586-024-08138-w**.
64 M. Speirs, S. J. O. Hardman, A. I. Iorgu, L. O. Johannissen, D. J. Heyes, N. S. Scrutton, I. V. Sazanovich and S. Hay, *J. Phys. Chem. Lett.*, 2023, **14**, 3236–3242.